Simultaneous estimation and correction of main field inhomogeneity

J. Sénégas[1], T. Knopp[2], and H. Eggers[1]

[1]Philips Research Europe, Hamburg, Germany, [2]University Luebeck, Luebeck, Germany

Introduction: Main field inhomogeneity, e.g. due to susceptibility differences, results in local off-resonance. The resulting image artefacts depend on the *k*-space trajectory used for acquisition and are more pronounced for long readout times. Existing correction schemes [1, 2] require a pre-measured map of the off-resonance frequencies as input. This calibration step costs additional scanning time, and may be useless in case of temporal variations of the local off-resonance, e.g. due to breathing. As an alternative, off-resonance estimation and correction can be achieved in one step, if two images at two different echo times are acquired simultaneously, at the cost of a computationally demanding non-linear reconstruction [3]. A novel, fast-converging algorithm to perform the joint reconstruction of off-resonance map and image is proposed herein and evaluated on spiral and echo planar imaging (EPI) data.

Theory: Accounting for off-resonance and neglecting relaxation, the signal s_{TE} received at echo time TE during an MRI experiment of length T_{AQ} can be described by:

$$s_{\mathrm{TE}}(t_i) = \int \rho(\mathbf{r}) \mathrm{e}^{-i2\pi f(\mathbf{r})(\mathrm{TE}+t_i)} \mathrm{e}^{-i2\pi \mathbf{k}(t_i).\mathbf{r}} d\mathbf{r} \,, \qquad (1)$$

where ρ denotes the transverse magnetization, f the off-resonance frequency, and **k** the *k*-space trajectory. After discretization, this relation can be decomposed into the two following vector equations:

$$\mathbf{s}_{\mathrm{TE}} = \mathbf{A}_{\mathbf{f}} \boldsymbol{\rho}_{\mathrm{TE}} \,, \qquad (2)$$

$$\boldsymbol{\rho}_{\mathrm{TE}} = \mathbf{P}_{\mathbf{f},\mathrm{TE}} \boldsymbol{\rho} \,. \qquad (3)$$

A denotes the encoding matrix comprising Fourier and off-resonance terms, and **P** is a diagonal matrix modelling the phase accumulation before the echo time TE. It is proposed to estimate **ρ** and **f** by means of a fixed-point iteration algorithm. One iteration consists of two steps. First, each echo image **ρ**(TE) is reconstructed on the basis of the current estimate of the off-resonance map, by solving Eq. 2. To perform this correction step, the CG algorithm with time segmentation proposed in Ref. [2] is applied. Then, the magnetization **ρ** and the off-resonance map **f** are estimated voxel-wise from the echo images **ρ**(TE) by solving Eq. 3 using a least-squares optimization algorithm. The resulting off-resonance map is unwrapped, and a mean-shift filter [4] is applied to reduce noise propagation. Image and off-resonance map updates are repeated until minimization of the L_2 norm r^2 of the residuals, given by:

$$r^2 = \sum_{\mathrm{TE}} \left\| \mathbf{s}_{\mathrm{TE}} - \mathbf{A}_{\mathbf{f}} \mathbf{P}_{\mathbf{f},\mathrm{TE}} \boldsymbol{\rho} \right\|^2 \qquad (4)$$

Methods: Convergence and precision of the fixed-point iteration algorithm were assessed on the basis of simulated spiral and EPI data for a 256×256 matrix size and a parabolic off-resonance map with values comprised between 0 and 175Hz. Spiral imaging in the brain was then performed on a 1.5T scanner (Achieva, Philips Medical Systems) with the following parameters: 18 interleaves, T_{AQ}=30ms, 256×256 matrix size, 250×250 FOV, TE_1=5ms, TE_2=6ms, TR= 1000ms, flip angle=70°. Reconstruction was performed by means of the fixed-point iteration algorithm, with 6 CG iterations and 36 time segments for the image reconstruction step.

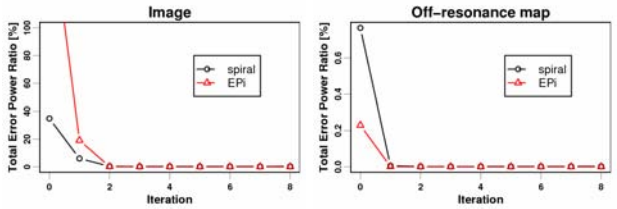

Fig 1: Evolution of the reconstruction error during the fixed-point iterations for the image and the off-resonance map.

Results: Fig. 1 shows the reconstruction error as a function of the iteration number for simulated data of a spiral trajectory with 12 interleaves and T_{AQ}=30ms, and of an EPI trajectory with 15 echoes and T_{AQ}=26.5ms. Convergence is reached after 8 iterations in both cases, with the main improvements occuring in the two first iterations. The field map was estimated with a precision below 0.5Hz, so that the final reconstruction error of the images is comparable to that of a reconstruction with known off-resonance map.

The reconstruction results for the spiral brain data are shown in Fig. 2. Estimating simultaneously the off-resonance map and the image allows to correct for the strong field inhomogeneity occurring e.g. at the air / tissue interface of the sinus cavities. As can be seen on the detailed view, most of the blurring present in the initial image, reconstructed without off-resonance correction, has been removed after convergence of the algorithm.

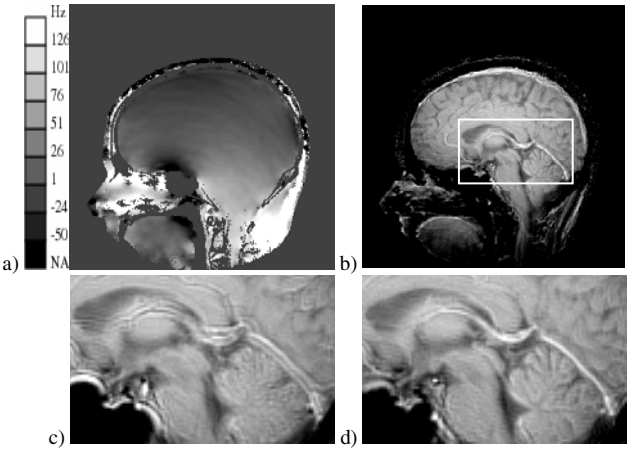

Fig. 2: Off-resonance map (a) and image (b) obtained after convergence of the joint estimation algorithm. Images corresponding to the initial (no correction) and last iteration, for the detail determined by the white rectangle, are shown in (c) and (d).

Discussion and conclusion: The rapid convergence of the fixed-point iteration algorithm was demonstrated with EPI and spiral imaging trajectories. The performance of the reconstruction loop is mainly governed by the iterative estimation of the off-resonance map. Low SNR or wrap errors may lead to reconstruction errors, although this can be compensated in part by spatial smoothing, at the cost of precision.

The proposed joint estimation approach enables the simultaneous measurement of the off-resonance map and imaging of the transverse magnetization by means of a rapid sequence having long readout times, such as EPI or spiral. Hence, the pre-measurement of the off-resonance map is not required anymore, which increases the robustness of such sequences against temporal variations of the main magnetic field and may reduce the overall acquisition time. As a side effect, rapid measurement of the off-resonance map based on EPI or spiral imaging also becomes possible, since the applied reconstruction removes geometric distortions and blurring. Applications requiring active shimming may benefit from such a rapid calibration scan.

References:

[1] Schomberg, TMI, 18(6):481–495 (1999). [2] Sutton et al, TMI, 22(2):178–188 (2003). [3] Sutton et al, MRM, 51:1194–1204 (2004). [4] D. Comaniciu et al, PAMI, 24(5):603–619 (2002).